Cell, Vol. 87, 675–686, November 15, 1996, Copyright ©1996 by Cell Press

Visualizing an Olfactory Sensory Map

Peter Mombaerts,* Fan Wang, Catherine Dulac, Steve K. Chao, Adriana Nemes, Monica Mendelsohn, James Edmondson, and Richard Axel
Department of Biochemistry
and Molecular Biophysics
Howard Hughes Medical Institute
and Center for Neurobiology and Behavior
College of Physicians and Surgeons
Columbia University
New York, New York 10032

Summary

We have developed a genetic approach to visualize axons from olfactory sensory neurons expressing a given odorant receptor, as they project to the olfactory bulb. Neurons expressing a specific receptor project to only two topographically fixed loci among the 1800 glomeruli in the mouse olfactory bulb. Our data provide direct support for a model in which a topographic map of receptor activation encodes odor quality in the olfactory bulb. Receptor swap experiments suggest that the olfactory receptor plays an instructive role in the guidance process but cannot be the sole determinant in the establishment of this map. This genetic approach may be more broadly applied to visualize the development and plasticity of projections in the mammalian nervous system.

Introduction

Mammals possess an olfactory system of inordinate discriminatory power (Shepherd, 1994; Buck, 1996). How is the diversity and specificity of olfactory perception accomplished? The initial step in the discrimination of odors involves the interaction of odor molecules with odorant receptors on the dendrites of olfactory sensory neurons. In mammals, the repertoire of odorant receptor genes may consist of as many as 1000 genes, each of which encodes a seven-transmembrane domain protein (Buck and Axel, 1991; Levy et al., 1991; Parmentier et al., 1992; Ben-Arie et al., 1994). Discrimination among odors requires that the brain determine which of the numerous receptors have been activated by a given olfactory stimulus. Individual olfactory neurons express only one or a small number of the 1000 receptor genes, such that neurons may be functionally distinct (Ngai et al., 1993; Ressler et al., 1993; Vassar et al., 1993). The problem in determining which receptors have been activated by an odorant can therefore be reduced to a problem of distinguishing which neurons have been activated.

As in other sensory systems, the pattern of projections of olfactory sensory neurons may provide a topographic map of receptor activation that defines the quality of a sensory stimulus. Analysis of the spatial patterns of receptor expression in the olfactory epithelium by in situ hybridization reveals that cells expressing a given receptor are restricted to one of four broad but circumscribed zones (Ressler et al., 1993; Vassar et al., 1993; Strotmann et al., 1992, 1994). The overriding feature of this organization, however, is that within a zone neurons expressing a given receptor are not topologically segregated, rather they appear randomly dispersed. In contrast, the axonal projections from neurons expressing a specific receptor converge upon two loci, or glomeruli, within the olfactory bulb (Ressler et al., 1994; Vassar et al., 1994). Neurons expressing a given receptor project to one medial and one lateral glomerulus, creating two mirror-image maps within each olfactory bulb. These observations are in accord with previous physiological experiments demonstrating that different odorants elicit spatially defined patterns of glomerular activity in the olfactory bulb (Stewart et al., 1979; Lancet et al., 1982; Kauer et al., 1987; Imamura et al., 1992; Mori et al., 1992; Katoh et al., 1993). The quality of an olfactory stimulus would therefore be encoded by the specific combination of glomeruli activated by a given odorant.

Evidence for the presence of a topographical map of receptor activation in the bulb derives largely from in situ hybridization experiments that detect the presence of specific receptor mRNAs at convergent loci in the olfactory bulb (Ressler et al., 1994; Vassar et al., 1994). The sensitivity of this approach does not permit the visualization of the projection pathways, but only identifies sites of axonal convergence. Moreover, these techniques do not afford resolution at the level of single axons. We therefore wished to develop a more sensitive genetic approach to visualize the projections of individual olfactory sensory neurons from the sensory epithelium to the olfactory bulb.

We have modified an olfactory receptor gene, P2, by targeted mutagenesis in the germline of mice. The P2 locus now encodes a bicistronic mRNA (Mountford and Smith, 1995) that allows the translation of the P2 receptor along with tau-lacZ (Callahan and Thomas, 1994), a fusion of the microtubule-associated protein tau with β-galactosidase. In these genetically altered strains of mice, olfactory neurons that transcribe the modified P2 allele also express tau-lacZ in their axons, permitting the direct visualization of the pattern of projections in the brain. We observe that neurons expressing the P2 receptor project to only two topographically fixed glomeruli of the 1800 glomeruli (Royet et al., 1988) in the mouse olfactory bulb. The pattern of convergence is absolute; stray axons projecting diffusely are not observed. These data provide direct support for a model in which a topographic map of receptor activation encodes odor quality in the olfactory bulb.

This genetic approach also permits the manipulation of genes responsible for the establishment and maintenance of the olfactory sensory map and may ultimately define how the topographic map is generated during development. We have substituted the P2 coding sequence with that of a second odorant receptor, M12.

*Present Address: The Rockefeller University, 1230 York Avenue, New York, New York 10021.

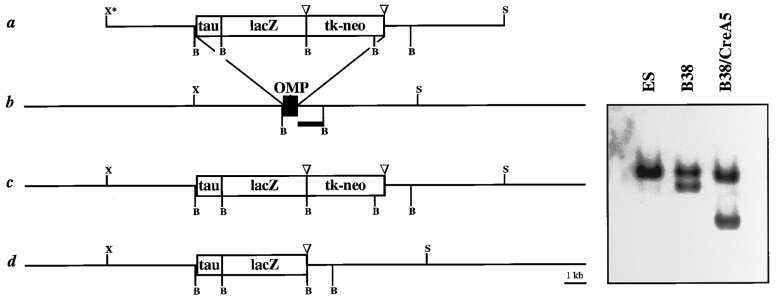

Figure 1. Targeted Mutagenesis of the *OMP* Locus

(Left) Schematic representation of the genetic strategy.

(a) Targeting vector OMP-KO-2. Tau-lacZ and LTNL (loxP-tk-neo-loxP) sequences replace 0.67 kb of the *OMP* gene shown in (b). The 5′ end is a XhoI site (X) and the 3′ end is an SphI site (S). The relevant BamHI sites (B) are indicated. Inverted triangles indicate *loxP* sites.

(b) Wild-type *OMP* locus. The black box labeled "OMP" indicates the sequences deleted following homologous recombination. The horizontal bar below the line represents the 3′ OMP probe, used to hybridize the Southern blot on the right.

(c) *OMP* locus after homologous recombination.

(d) *OMP* locus after Cre-mediated site-specific recombination. A single *loxP* site is left behind.

(Right) Southern blot of genomic DNA from wild-type ES cells, targeted clone B38, and Cre-treated subclone B38/CreA5. DNA was cut with BamHI and hybridized with the 3′ OMP probe. The upper band in lane ES represents the wild-type allele (see [b], 2.0 kb), the lower band in lane B38 is the targeted allele (see [c], 1.8 kb), and the lower band in lane B38/CreA5 is the allele after Cre-excision (see [d], 1.3 kb).

This receptor swap alters the pattern of projections, suggesting that the olfactory receptor plays an instructive role in the guidance process but cannot be the sole determinant in axon targeting.

Results

The OMP-tau-lacZ Mouse

We wished to develop a genetic approach to visualize the axonal projections from specific subpopulations of olfactory neurons. The tau-lacZ fusion protein is efficiently transported down axonal processes of Drosophila neurons (Callahan and Thomas, 1994). Initial experiments were designed to determine whether this protein could also be detected in axons of mouse olfactory neurons, which are considerably longer than an entire fly. We therefore generated a mouse strain in which the sequences encoding the olfactory marker protein (OMP) (Buiakova et al., 1994) are replaced by tau-lacZ. OMP is a protein of unknown function that is expressed at high levels in all mature olfactory sensory neurons (Farbman and Margolis, 1980). A targeting vector OMP-KO-2 (Figure 1) was designed such that homologous recombination at the *OMP* locus would result in the replacement of the single exon of *OMP* with tau-lacZ coding sequences. Downstream of tau-lacZ, this vector contains an expression cassette that includes a 5′ *loxP* site (Hoess et al., 1982), the herpes simplex virus *thymidine kinase* gene (*tk*) (McKnight, 1980), the *neomycin resistance* gene (*neo*) (Adra et al., 1987), and a 3′ *loxP* site (an LTNL cassette for loxP-tk-neo-loxP). When this targeting vector was electroporated into ES cells, homologous recombination at the *OMP* locus was observed in 25% of the G418-resistant clones (Figure 1). One targeted ES clone (B38) was expanded and transiently transfected with a plasmid encoding the Cre recombinase driven by the cytomegalovirus promoter (pBS185) (Sauer and Henderson, 1990). Following transfection, cells were negatively selected with ganciclovir to enrich for clones that had undergone Cre-mediated excision of the *tk-neo* expression cassette. Southern blot analysis identified 12 out of 55 ganciclovir-resistant colonies that had undergone site-specific recombination. One clone (B38/CreA5) was injected into C57BL/6 blastocysts, and most male chimeras transmitted the mutation through the germline.

A whole mount preparation from a mouse heterozygous for the OMP-tau-lacZ mutation reveals the labyrinthine convolutions or turbinates that characterize the olfactory epithelium on the medial aspect of the nasal cavity (Figure 2A). Intense blue staining with X-Gal, indicative of lacZ activity, is observed throughout the epithelium lining each of the turbinates. A sharp border separates the OMP negative respiratory epithelium from the OMP positive sensory epithelium. In preparations in which the septum is left intact, staining is also observed in sensory neurons of the vomeronasal and septal organs (Figure 2B). The vomeronasal organ is a functionally distinct sensory epithelium (Figure 2C) that is activated by pheromones and projects to the anatomically distinct accessory olfactory bulb (Figure 2D).

Intense staining is observed in the olfactory sensory axons that project through the cribriform plate into the olfactory bulb. Sections through the olfactory epithelium and bulb, followed by staining with X-Gal, reveal densely packed sensory neurons in the epithelium (data not shown) that project axons to the olfactory bulb (Figure 2E). The axons terminate within discrete structures, the glomeruli, where individual sensory axons synapse with the dendrites of mitral cells (Figures 2E and 2F). A dorsal view of the bulb reveals sensory fibers terminating in the glomeruli of the main olfactory bulb and a distinct collection of fibers from the vomeronasal organ entering the accessory olfactory bulb (Figure 2D). These observations demonstrate that tau-lacZ is efficiently transported down the axons of olfactory sensory neurons, allowing the visualization of axon termini in individual glomeruli. Moreover, the expression of tau-lacZ does not appear to alter the gross pattern of neuronal connectivity between the epithelium and the bulb.

Visualizing Neurons Expressing the P2 Receptor

We next generated mice in which only a subpopulation of olfactory sensory neurons transcribing a specific receptor, P2, also express the fusion protein tau-lacZ. In these mice, it is possible to visualize the pattern of receptor gene expression in individual neurons in the epithelium and the pattern of projections of these neurons in the olfactory bulb. To restrict the expression of

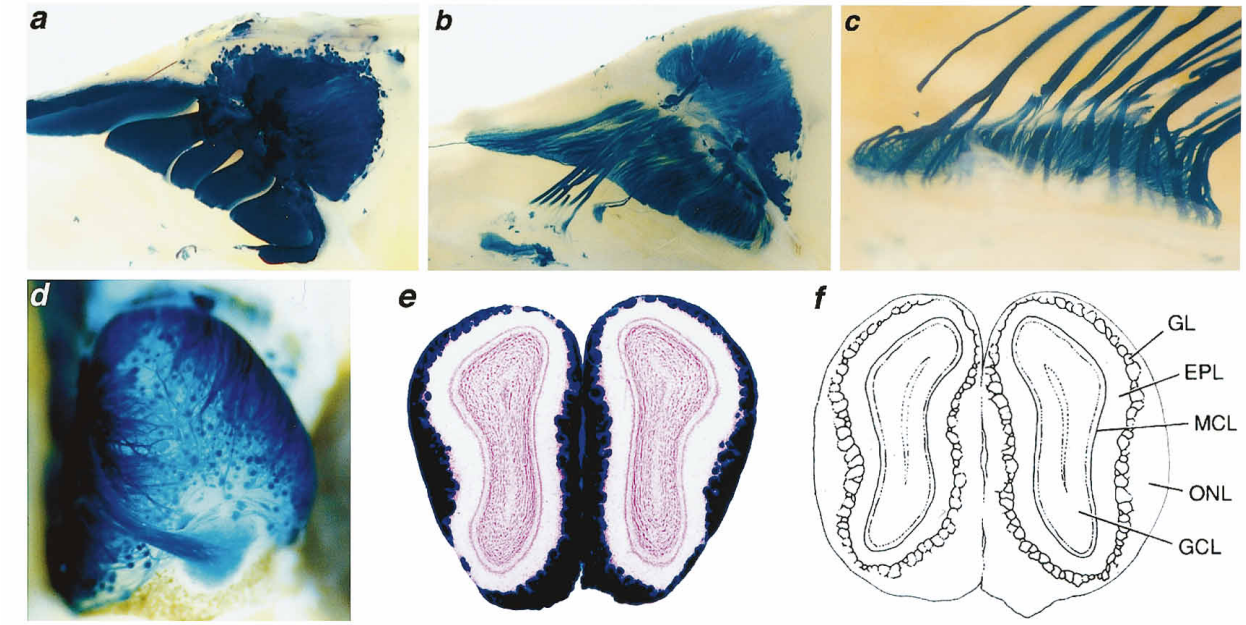

Figure 2. OMP-tau-lacZ Mice, Stained with X-Gal

(a) Whole mount view of the wall of the nasal cavity and the medial aspect of the olfactory bulb. (b) Whole mount view of the nasal septum and the medial aspect of the bulb. (c) Whole mount higher power view of the vomeronasal organ. (d) Whole mount view of the dorsal-posterior aspect of the olfactory bulb. (e) Coronal section through the right and left olfactory bulbs counterstained with neutral red. (f) Schematic diagram of coronal section through the olfactory bulbs. Orientation of (a) and (b): anterior to the left, dorsal at top; the right half of a mouse head is shown. Orientation of (d): medial to the left, anterior at top. (a) Cell bodies, dendrites and axons are stained intensely such that the epithelium (left) and the bulb (top right) appear deeply blue. (b) The nasal septum, which divides the nasal cavity along the midline, contains three olfactory structures: the main olfactory epithelium (right), the vomeronasal organ (bottom left), and the septal organ (visible as a small triangle in between the former two structures). The bulb is at the top right. (c) The vomeronasal organ also contains OMP expressing olfactory neurons, whose axonal processes fasciculate in the septum. (d) Fascicles of blue axons from the main olfactory epithelium terminate in distinct glomeruli in the bulb. The axons of vomeronasal neurons run on the medial side of the bulb and fan out in the accessory olfactory bulb, visible at the bottom as a homogeneously blue structure. (e) Coronal sections reveal staining in the blue outer nerve layer and the glomerular layer which contain, respectively, axons and axon terminals of olfactory neurons. Neutral red stains the cell bodies of periglomerular cells (adjacent to the glomeruli), mitral cells and granular cells. (f) ONL, outer nerve layer; GL, glomerular layer; EPL, external plexiform layer; MCL, mitral cell layer; GCL, granular layer. Heterozygous mice of the B38/CreA5 line were 3–8 weeks old, except (b), 13 days old and (d), 9 days old. X-Gal staining was performed for 1–2 hr.

tau-lacZ to the subpopulation of sensory neurons that express the odorant receptor P2, it is necessary to place tau-lacZ under the control of P2 regulatory sequences, such that cells expressing P2 will also express tau-lacZ. However, the elements regulating receptor gene expression have not yet been identified. We therefore chose to introduce tau-lacZ into the P2 locus by homologous recombination in ES cells. A gene-targeting approach in which the P2 coding sequence is simply replaced by tau-lacZ would eliminate P2 receptor expression from the modified allele. However, olfactory neurons express a receptor from only one of the two alleles (Chess et al., 1994). Therefore, in this targeting strategy, cells expressing the modified P2 allele would express tau-lacZ, but not receptor. Conversely, cells expressing the wild-type P2 allele would express receptor, but not tau-lacZ. To assure that cells expressing tau-lacZ also express a functional P2 receptor, we designed a targeting vector that would result in a bicistronic mRNA (Mountford and Smith, 1995). A genomic clone containing the P2 receptor gene was modified by the insertion of a cassette immediately 3′ of the P2 stop codon (Figure 3). This cassette consists of two parts: an internal ribosome entry site (IRES) from the encephalomyocarditis virus (Kim et al., 1992) driving translation of the tau-lacZ sequences, followed by LTNL (loxP-tk-neo-loxP). Cells expressing the modified P2 allele should now express the P2 receptor along with tau-lacZ. The targeting vector was electroporated into ES cells and G418-resistant clones were analyzed by Southern blot hybridization. Four of 720 G418-resistant clones resulted from homologous recombination at the P2 locus (Figure 3). Targeted ES clones were then transiently transfected with a vector directing expression of the Cre recombinase (pBS185) resulting in deletion of the *tk-neo* sequences, leaving only a single *loxP* site. Five of 24 ganciclovir-resistant subclones of clone FD257 resulted from Cre-mediated site-specific recombination. Removal of the selectable markers ensures that the modified P2 locus is free of exogenous promoter elements that may affect P2 expression. These ES clones were then introduced into blastocysts to generate chimeric mice, and germ line transmission was obtained with two clones (FD257/Cre7 and FK290/Cre53).

Whole mount analysis of mice heterozygous for the P2-IRES-tau-lacZ mutation reveals a subpopulation of

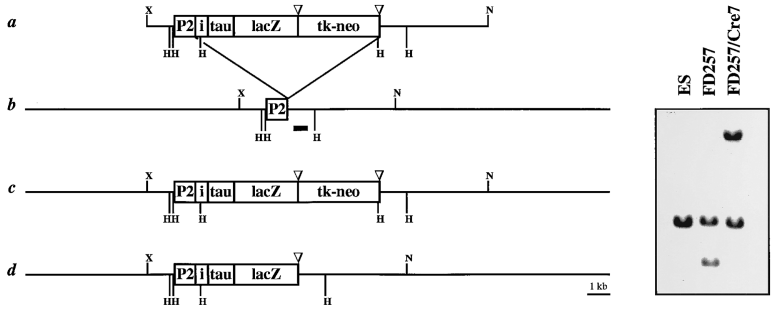

Figure 3. Targeted Mutagenesis of the P2 Locus

(Left) Schematic representation of the genetic strategy. (a) Targeting vector P2-KO-13. The 5′ end is a XhoI site (X), the 3′ end is an NcoI site (N). The relevant HindIII sites (H) are indicated. Inverted triangles indicate *loxP* sites. (b) Wild-type P2 locus. The coding sequence of the P2 gene consists of one exon. The horizontal bar below the line represents the 3′ P2 probe used to hybridize the Southern blot on the right. (c) P2 locus after homologous recombination. (d) P2 locus after Cre-mediated site-specific recombination. (Right) Southern blot of genomic DNA from wild-type ES cells, targeted clone FD257, and Cre-treated subclone FD257/Cre7. DNA was cut with HindIII and hybridized with the 3′ P2 probe. The upper band in lane ES represents the wild-type allele (see [b], 2.2 kb), the lower band in lane FD257 is the targeted allele (see [c], 1.5 kb), and the upper band in lane FD257/Cre7 is the allele after Cre-excision (see [d], 6.5 kb).

sensory neurons whose dendrites, cell bodies, and axons exhibit blue color after staining with X-Gal (Figure 4). The blue axons are readily visualized as they emerge from the epithelium and pass through the cribriform plate into the olfactory bulb where they converge on two glomeruli: one on the medial and one on the lateral aspect of the bulb.

In initial experiments, we demonstrated that the pattern of expression of the modified P2-IRES-tau-lacZ allele mimics that of the wild-type P2 allele. Neurons expressing a given receptor are topographically segregated within one of four zones in the olfactory epithelium (Ressler et al., 1993; Vassar et al., 1993). In situ hybridization to coronal sections through the olfactory epithelium of wild-type mice reveals P2 expressing cells within the third zone (zone II in Ressler et al., 1993) (data not shown). Since a neuron expressing P2 is expected to transcribe this gene from only one of the two alleles, X-Gal staining in a P2-IRES-tau-lacZ heterozygous mouse will only identify cells expressing the modified P2 allele. In adjacent sections, in situ hybridization with a digoxigenin-labeled P2 antisense RNA probe identifies cells expressing P2 RNA from the modified allele as well as cells expressing P2 from the unaltered allele. We observe similar spatial patterns of P2 in situ hybridization and lacZ staining in alternate sections of the olfactory epithelium (Figures 5A and 5B). Moreover, the topographic pattern of P2 expression in the P2-IRES-tau-lacZ mice is similar to that observed in wild-type mice (Figures 5C and 5D), suggesting that expression of the P2-IRES-tau-lacZ allele is unaltered by these genetic manipulations.

In heterozygotes, which carry one wild-type P2 allele and one modified P2-IRES-tau-lacZ allele, the number of lacZ positive cells is about half of the total number of P2 expressing cells determined by in situ hybridization with P2 probes (Figures 5A and 5B). In homozygotes, however, the number of P2 expressing cells equals the number of lacZ expressing cells (data not shown). These data suggest that cells expressing the wild-type P2 allele do not express the modified P2-IRES-tau-lacZ allele, providing further support for monoallelic expression at the olfactory receptor loci (Chess et al., 1994).

Analysis of the olfactory bulb, either in whole mount preparations or after sectioning, permits the direct visualization of the axonal projections from neurons expressing P2-IRES-tau-lacZ. On the medial aspect of the bulb, the blue axons converge upon a single glomerulus (Figure 4). On the lateral half of the olfactory bulb, axons converge to a single, more dorsally and anteriorly placed glomerulus (data not shown). A pattern of one medial and one lateral blue glomerulus has been observed in 35 out of 37 heterozygous and homozygous mice. A small fraction of the blue fibers (<5%) project to a third glomerulus in the immediate vicinity of one of the two P2 glomeruli. In 2 of 37 mice, projection to an additional glomerulus at that location is observed. This minor variance is also detected by in situ hybridization experiments in wild-type mice (data not shown). At this level of resolution, we see no stray fibers: all axons appear to project to the two or three glomeruli we have identified. The positions of these glomeruli are relatively constant in all mice examined. This conclusion is strengthened by in situ hybridization with probes for two receptors, M50 and P2, which reveal that the relative positions of two distinct glomeruli with respect to one another remain constant in different animals (our unpublished data).

The ability to visualize neurons expressing the P2 receptor also allows us to observe the generation of the topographic map over developmental time. Neurons expressing P2-IRES-tau-lacZ are first visualized at embryonic day 12.5. At this time, blue neurons are observed that have not yet elaborated axons (data not shown). Convergence of axons from P2 expressing neurons is apparent from embryonic day 16.5, and the medial and lateral glomeruli are clearly visible at birth (Figure 6). Moreover, the relative positions of these glomeruli remain fixed throughout the life of the organism.

It is important to establish that in a P2-IRES-tau-lacZ heterozygous mouse, blue neurons expressing the P2-IRES-tau-lacZ allele project their axons to the same glomeruli as neurons expressing the wild-type P2 allele. We therefore prepared 20 μm serial cyrostat sections through the entire olfactory bulb. Alternate sections were either stained with X-Gal or subjected to in situ hybridization with ^{33}P-labeled antisense P2 RNA probes (Figures 5E–5H). The presence of small amounts of receptor RNA within the terminals of sensory axons in the olfactory bulb allows us to observe the sites of convergence of the projections of neurons expressing P2 mRNA. X-Gal staining identifies the axonal projections from neurons expressing the P2-IRES-tau-lacZ allele. The in situ hybridization and X-Gal staining identify the

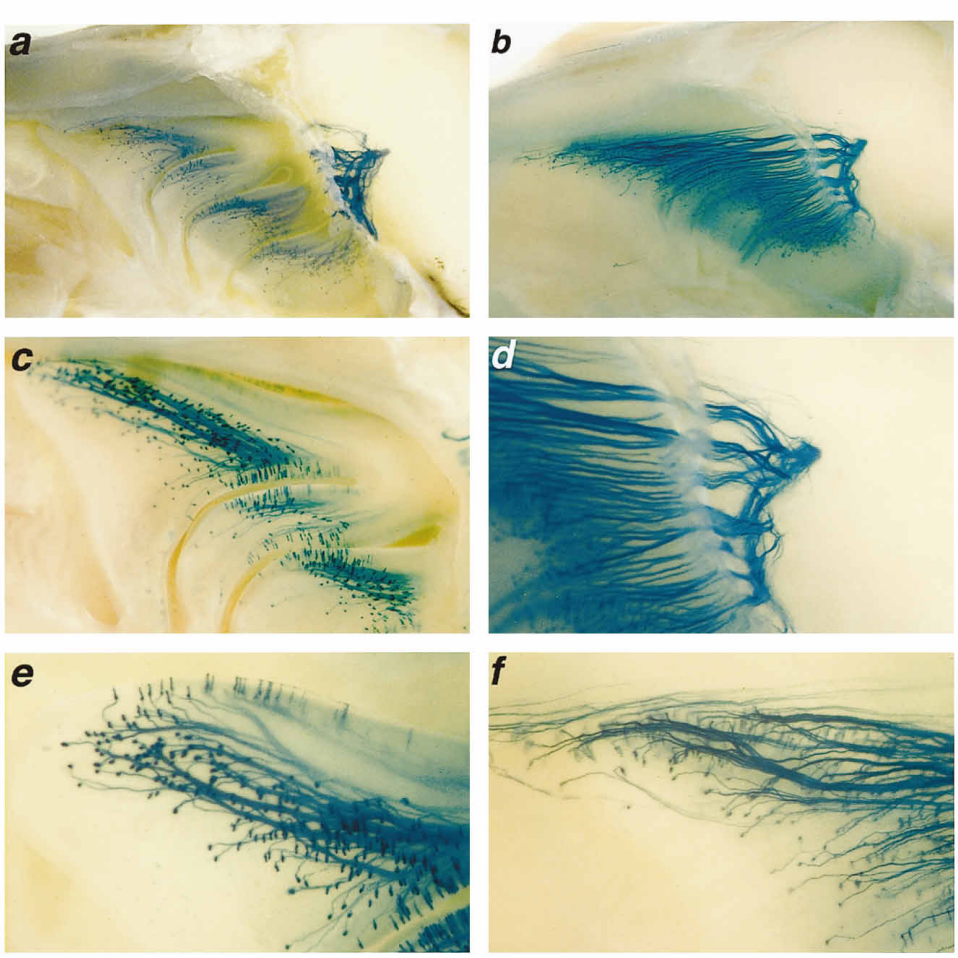

Figure 4. P2-IRES-tau-lacZ Mice, Stained with X-Gal

(a) Whole mount view of the wall of the nasal cavity and the medial aspect of the bulb (4-week-old mouse). (b) View of the nasal septum and the medial aspect of the bulb (4-month-old mouse). (c) Higher power view on the turbinates. (d) Higher power view of glomerulus. (e) Higher power view of epithelium. (f) Higher power view of neurons within the septum. (a) Blue neurons are distributed in a single zone (zone 3) in the sensory epithelium. Their axons converge on a single glomerulus on the medial aspect of the bulb, close to the cribriform plate. The lateral side of the bulb is not visible in this view. The entire olfactory epithelium is faintly blue-green colored, due to overstaining necessary to visualize the glomerulus. As the septum is removed, the axons on the bulb are broken off. (b) Blue neurons in the septum are also zonally restricted. (c) The neurons are located in a narrow zone (zone 3) in the epithelium. (d) Close up of specimen shown in (b). Axons and axon bundles are contiguous between the septum (left) and the bulb (right). No stray axons are visible at the level of the bulb. The cribriform plate, which separates the nasal from the cranial cavity, is cut during the dissection and is visible as an opaque vertical band. (e and f) Individual neurons are visualized with staining of the dendrite, cell body, and axon. Heterozygous mice of the FD257/Cre7 line were between 3 and 12 weeks old. X-Gal staining was carried out for 2–16 hr.

same glomeruli in alternate sections of the olfactory bulb (Figures 5E–5H). These data demonstrate that neurons expressing the P2-IRES-tau-lacZ allele project to the same glomeruli as neurons expressing the unmodified P2 allele. Thus, this genetic alteration of the P2 receptor locus does not alter the pattern of expression of P2 receptor in the epithelium or the pattern of projections to the olfactory bulb. Therefore, the pattern of P2-IRES-tau-lacZ expression accurately represents the convergence of axons from neurons expressing the P2 receptor on two topographically fixed glomeruli in the mouse olfactory bulb.

We emphasize that interpretation of the observations in these genetically altered mice requires control experiments that examine the pattern of expression and pattern of projections of neurons expressing the wild-type allele compared with the modified allele. These patterns are superimposable for cells expressing the wild-type P2 allele or the P2-IRES-tau-lacZ allele. However, olfactory neurons from strains of mice expressing IRES-tau-lacZ introduced into another receptor gene, M12, exhibit altered patterns of expression in the epithelium and altered glomerular targets in the bulb (data not shown). The aberrant projection of neurons expressing the M12-IRES-tau-lacZ allele may be the consequence of altered topographic patterns of expression in the epithelium.

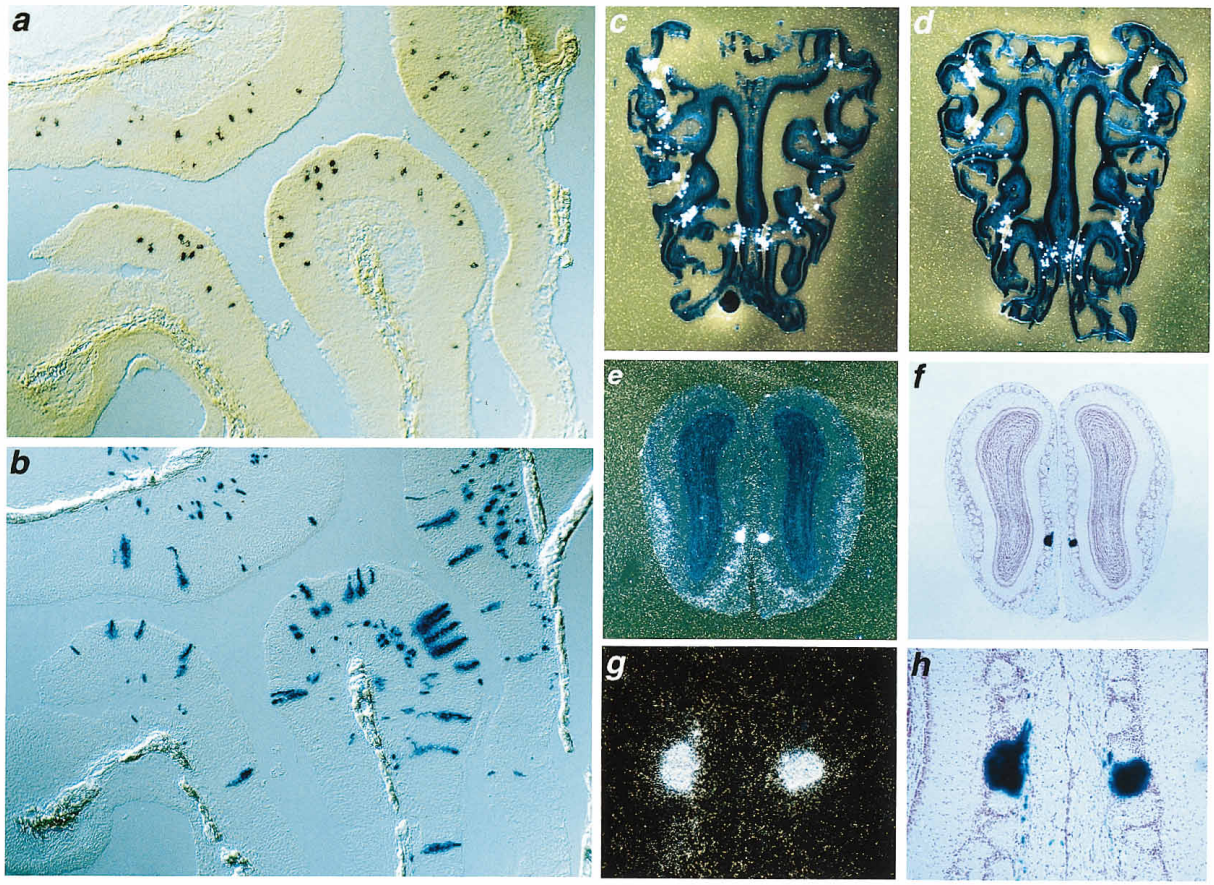

Figure 5. In Situ Hybridization with P2 Probe and X-Gal Staining of Coronal Sections through Turbinates and Olfactory Bulb

(a and b) Alternate coronal sections through turbinates of a P2-IRES-tau-lacZ heterozygous mouse, subjected to in situ hybridization with digoxigenin-labeled P2 probe (a) and X-Gal staining (b). (c and d) Coronal sections through turbinates of a wild-type (c) and a heterozygous mouse (d), hybridized with a ^{33}P-labeled P2 probe; (e and f) Adjacent coronal sections through olfactory bulbs of a heterozygous mouse, subjected to in situ hybridization with a ^{33}P-labeled P2 probe [e]) and X-Gal staining (f). (g and h) Higher power view of glomeruli in (e) and (f). (a and b) The pattern of cells labeled by either in situ hybridization or X-Gal staining is similar. In this heterozygous mouse, roughly twice as many cells are visualized by in situ hybridization as compared to X-Gal staining. Note that in situ hybridization reveals only the cell bodies of P2 expressing neurons, whereas X-Gal staining identifies various sections through dendrites, cell bodies, or axons, and only cell bodies should therefore be counted. The septum is located on the right. (c and d) A radial zone of P2 expressing cells is observed in coronal sections. The patterns are similar between the wild-type and the heterozygous mouse. (e and f) In serial coronal sections of the bulb, glomeruli identified by in situ hybridization with the P2 probe are identical to those stained with X-Gal. The location of these medial glomeruli is bilaterally symmetric. (g and h) Higher power magnification identifies the stained areas as glomeruli. In (h), glomeruli can be discerned as white areas surrounded by a thin layer of red stained cell bodies of periglomerular neurons.

Alternatively, if odorant receptor is important for appropriate axon targeting, altered levels of receptor may effect the pattern of projections to the olfactory bulb.

The Effect of a Receptor Swap on Axonal Projections

The precision of the topographic map of sensory projections implies a tight linkage between the choice of a specific odorant receptor and the choice of a glomerular target. The genetic approach we have developed to visualize these projections allows us to examine the relationship between receptor expression and axon targeting. In initial experiments, we have determined the consequences of substituting the P2 receptor coding region with the corresponding sequences from a second receptor, M12. A gene targeting strategy was devised to ensure that expression of the M12 receptor was under the control of the P2 regulatory sequences. Neurons that choose to express this modified P2 allele instead express M12 along with tau-lacZ (M12→P2-IRES-tau-lacZ), allowing the direct visualization of the consequences of a receptor swap on the pattern of axonal projections.

One extreme model for the formation of the topographic map invokes the odorant receptor as the sole determinant of axon targeting. In such a model the replacement of P2 with M12 receptor sequences should drive the blue axons to the wild-type M12 glomeruli. At the other extreme, the odorant receptor may play no

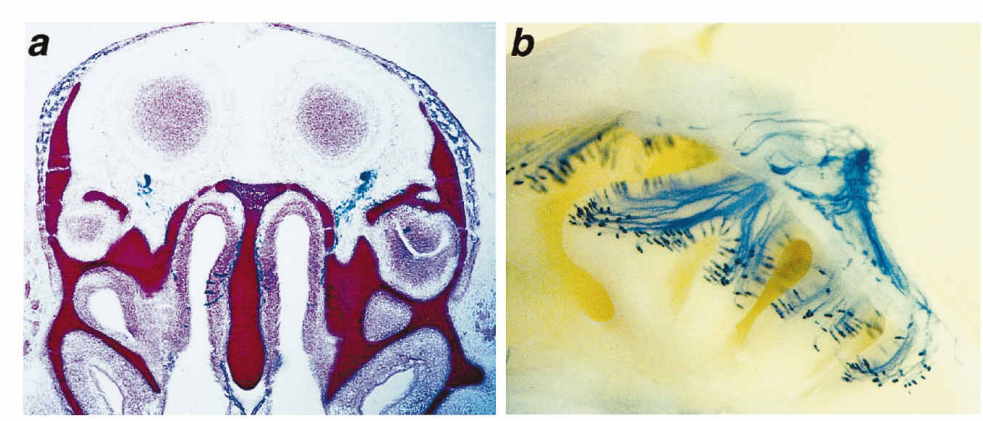

Figure 6. Axonal Convergence of P2 Expressing Neurons Is Apparent at Birth

(a) Coronal section of a newborn mouse, stained with X-Gal and counterstained with neutral red. A few blue neurons can be seen in the olfactory epithelium lining both sides of the septum. One blue glomerulus is visible on the lateral side of each olfactory bulb. Their location is bilaterally symmetric. The medial glomeruli are more posterior and therefore not present in this section.

(b) Whole mount view of turbinates (left) and medial side of bulb (right). Cell bodies of individual neurons can be discerned in a zonally restricted fashion. Blue axons can be seen at the level of the epithelium projecting toward the bulb because the epithelium is more translucent than in older animals.

role in the targeting process, such that cells expressing the M12→P2 swap should maintain their projections to the wild-type P2 glomeruli.

The targeting vector encoding M12→P2-IRES-tau-lacZ was constructed by the substitution of the P2 coding sequences with those of the M12 receptor (Figure 7A). The P2 sequences were deleted between the start and stop codons to retain the P2 5′ and 3′ untranslated sequences, along with the flanking P2 sequences, and were replaced with the M12 coding sequence. The M12 sequence contains a nine amino acid hemagglutinin epitope between the second and third amino acid. Downstream of the stop codon of M12, we inserted the IRES-tau-lacZ/loxP-tk-neo-loxP cassette. This targeting vector was electroporated into ES cells and one G418-resistant clone that resulted from homologous recombination at the P2 locus was identified. This clone was transiently transfected with a vector directing the expression of the Cre recombinase to delete the *tk-neo* sequences, and germline chimeras were generated.

In wild-type mice, M12 expressing neurons project axons to two glomeruli that reside dorsally in the posterior aspect of the olfactory bulb. The M12 glomeruli reside at fixed positions quite distant from the P2 glomeruli, which occupy a more ventral and anterior location (Figure 7B). Moreover, the M12 gene resides on a different chromosome than P2 (data not shown) and is expressed in a different epithelial zone (zone 4) than P2 (zone 3).

Whole mount analysis of mice either heterozygous or homozygous for the M12→P2-IRES-tau-lac-Z mutation reveals the presence of blue neurons in the P2 zone and the convergence of blue axons on one medial and one lateral glomerulus, which occupy a ventral and anterior position (a homozygous mouse is shown in Figure 7C). Although these glomeruli are clearly distant from the wild-type M12 glomeruli, it is not possible by whole mount analysis alone to determine whether they are coincident with the wild-type P2 glomeruli. Serial cryostat sections were therefore prepared through the entire olfactory bulb from four heterozygous M12→P2-IRES-tau-lacZ mice. Alternate sections were either stained with X-Gal or subjected to in situ hybridization with a ^{33}P-labeled antisense P2 RNA probe. In situ hybridization identifies the projections from neurons expressing the wild-type P2 allele. X-Gal staining identifies the axonal projections from neurons expressing the M12→P2-IRES-tau-lacZ allele. We find that neurons expressing the M12→P2-IRES-tau-lacZ allele project to glomeruli very near to, but distinct from, the wild-type P2 glomeruli. The M12→P2 glomeruli reside at a position ~200 μm (two glomerular widths) posterior to the wild-type P2 glomeruli and roughly in the same dorsoventral plane (Figures 7D–7G). These relative positions are maintained on both the medial (Figures 7F and 7G) and lateral (Figures 7D and 7E) aspect of the bulb and are consistently observed in the right and left bulb in each of the four mice studied. The probability that the M12→P2 glomeruli would randomly reside this close to the P2 glomeruli is ~0.03. It should be emphasized that the position of the M12→P2 glomeruli, near to but distinct from the P2 glomerulus, does not reflect animal-to-animal variance. In all P2-IRES-tau-lacZ mice studied, the neurons expressing the modified P2 allele project to the same glomeruli as do neurons expressing the wild-type P2 allele (Figures 5E–5H). In contrast, in four M12→P2-IRES-tau-lacZ mice, neurons expressing the modified M12→P2 allele project to different glomeruli than do neurons expressing the wild-type P2 allele. Thus, the analysis of heterozygous animals provides an internal control for slight variations in the map between different animals.

Thus, the substitution of P2 coding sequences by those of M12 results in the convergence of axons to topographically fixed glomeruli distant from the wild-type M12 glomeruli, but very close to the wild-type P2

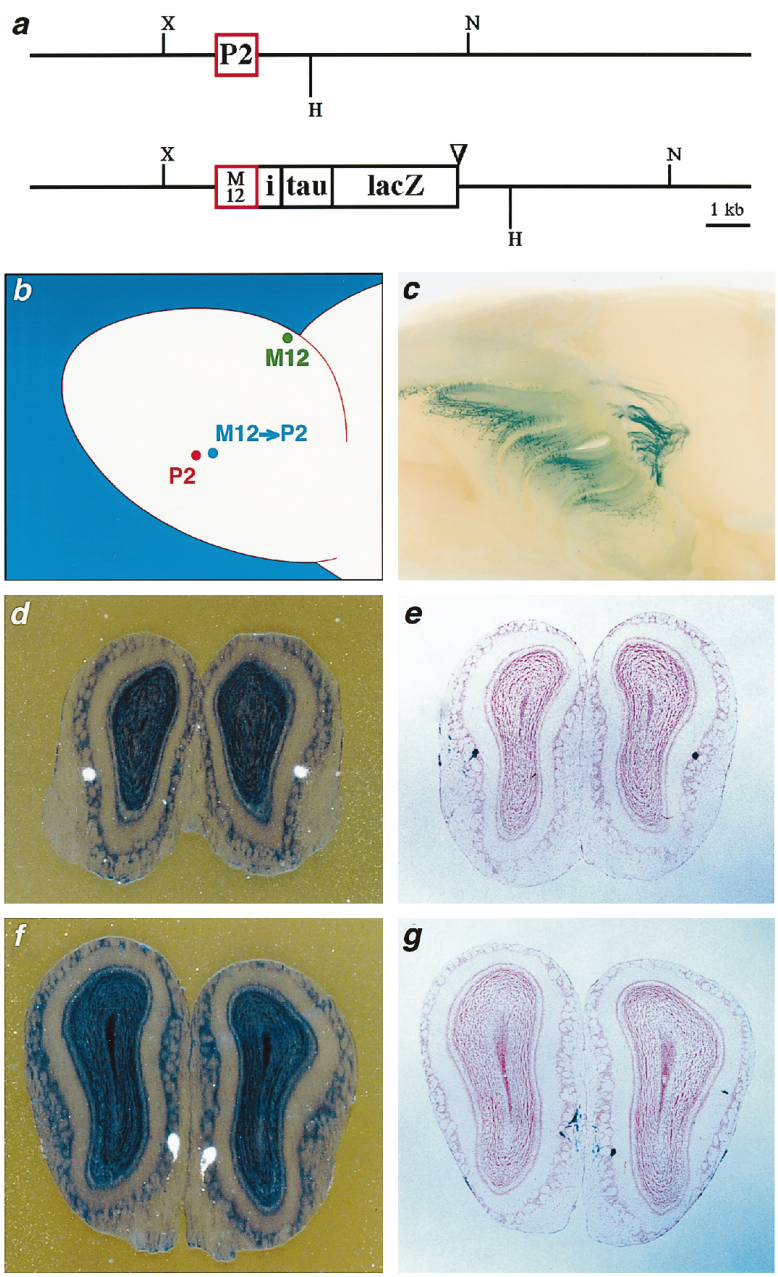

Figure 7. M12→P2-IRES-tau-lacZ Mouse

(a) Comparison of the wild-type P2 locus (top) and the M12→P2-IRES-tau-lacZ mutation, after homologous recombination and Cre-excision of the selectable markers (bottom). The genetic manipulation results in the substitution of the P2 coding sequence with that of the odorant receptor M12 (red box). X, XhoI; H, HindIII; N, NcoI.

(b) Schematic diagram of the right olfactory bulb, view on the medial aspect. The locations of the P2 (red), M12 (green), and M12→P2 (blue) glomeruli are indicated. A similar arrangement is found on the lateral aspect of the bulb (not shown), implying a mirror-type of symmetry in the bulb.

(c) Whole mount view of a five week old M12→P2-IRES-tau-lacZ homozygous mouse. Blue neurons are located in zone 3 and project their axons to a single glomerulus on the medial aspect of the bulb.

(d–g) Sections of the olfactory bulb of a M12→P2-IRES-tau-lacZ heterozygous mouse. In situ hybridization (d and f) identifies the glomeruli to which the neurons expressing the wild-type P2 allele project. X-Gal staining (e and g) identifies the glomeruli to which the neurons expressing the M12→P2 allele project. It is important to note that there are approximately ten 20 μm sections between the sections exhibiting positive glomeruli by in situ hybridization and X-Gal staining, both on the lateral aspect (d and e) and the medial aspect of the bulb (f and g). Thus, the M12→P2 glomeruli are located 200 μm (two glomerular widths) posterior to P2 glomeruli. Moreover, sections immediately adjacent to the lacZ positive M12→P2 glomeruli are negative for P2 expression; sections adjacent to the P2 glomeruli are negative for lacZ staining.

glomeruli. These results suggest that the odorant receptor itself cannot be the sole determinant of axonal targeting. However, the segregation of the M12→P2 glomeruli from the P2 glomeruli suggests that the receptor may be one determinant in a more complex guidance process.

Discussion

Visualizing an Olfactory Sensory Map

We have developed a genetic approach to visualize axons from olfactory sensory neurons expressing a given odorant receptor as they project to the olfactory bulb. The experimental strategy involves the manipulation of an olfactory receptor gene expressed in a restricted subpopulation of sensory neurons, such that the faithful expression of this modified allele leads to the transcription of a bicistronic message that also includes tau-lacZ. Our data, along with in situ hybridization analysis of receptor mRNA in the bulb (Ressler et al., 1994; Vassar et al., 1994), demonstrate that neurons expressing a given receptor, and therefore responsive to a given odorant, project with precision to 2 of the 1800 glomeruli within the olfactory bulb. Since the positions of individual glomeruli are topographically defined, the bulb provides a spatial map that identifies which of the numerous receptors have been activated within the sensory epithelium. The quality of an olfactory stimulus would therefore be encoded by the specific combination of glomeruli activated by a given odorant. This model for olfactory

discrimination is consistent with previous physiological studies (Stewart et al., 1979; Lancet et al., 1982; Kauer et al., 1987; Imamura et al., 1992; Mori et al., 1992; Katoh et al., 1993) suggesting that glomeruli represent functional units such that different odorants elicit spatially defined patterns of glomerular activity in the olfactory bulb.

The observation that each of the 1000 different subpopulations of sensory neurons projects with precision to a small number of topographically fixed glomeruli poses an interesting but complex problem in axon guidance: how do neurons expressing a given receptor know which target to project to in the bulb? In this study, we describe a genetic approach to address how this precise topographic map is established (see also Mombaerts, 1996). More specifically, we have asked whether the receptor plays a role in the guidance process.

The Establishment of the Topographic Map

What are the determinants guiding the projections of sensory axons? In other sensory systems, guidance molecules during development, along with activity-dependent refinement, achieve a precision of connections between the periphery and the brain (Constantine-Patton et al., 1990; Woolsey, 1990; Goodman and Shatz, 1993). Two observations argue strongly for the existence of spatial cues in the bulb that are recognized by a specific complement of guidance receptors in sensory axons and direct olfactory projections to appropriate glomerular positions. First, the topographic map, in which each of the 1000 different subpopulations of sensory neurons project to only two glomeruli, is fixed in all organisms within a species. Moreover, the relative positions of multiple distinct glomeruli are conserved in different organisms (S. Chao and R. A., unpublished). Whereas guidance mechanisms can be envisaged that exploit synchronous activation to effect the segregation of axons from neurons bearing the same receptor, it is difficult to invoke pure activity-dependent mechanisms that precisely determine 1800 positions of axonal convergence in the bulb in a stereotyped fashion. Second, we observe the convergence of axons at early times in development prior to the formation of a glomerulus (data not shown). Although these data do not exclude activity-dependent processes as a mechanism of spatial refinement, they strongly suggest the existence of spatial cues in the bulb that guide axons to the 1800 precise loci.

Is the odorant receptor a determinant of the guidance process in sensory axons? If the receptor does play a role in the generation of the topographic map, then sensory neurons must express olfactory receptors prior to target selection in the bulb. This would eliminate an alternative model in which immature neurons, not yet expressing receptor, randomly project axons to the bulb. Positional information in the bulb may then elicit a retrograde signal that directs the expression of specific receptor genes. This retrograde model is unlikely since in embryonic P2-IRES-tau-lacZ mice we observe blue neurons expressing receptor that have not yet elaborated axons. Similar conclusions emerge from developmental analysis of receptor expression by in situ hybridization (Strotmann et al., 1995; Sullivan et al., 1995). Thus, it is likely that neurons first express receptor and only later project to specific targets in the bulb.

A tight linkage is observed between the choice of an odorant receptor and the sites of axonal convergence in the olfactory bulb. Perhaps the most parsimonious model would argue that the odorant receptor is expressed on dendrites and recognizes odors in the environment, and is also expressed on axon termini where it would recognize a set of guidance cues, distinct from odorous ligands, expressed by bulbar cells. In this manner, an olfactory neuron would be afforded a distinct identity that dictates the nature of the odorants to which it responds, as well as the glomerular target to which its axons project. The results of the receptor swap experiment suggest that the odorant receptor indeed plays a role in the guidance process. However, the receptor cannot be the sole determinant of axonal targeting, rather it is likely to be one component in a more complex guidance process.

We have replaced the P2 receptor coding sequence with the coding sequence of M12 (M12→P2) to observe the consequences of altering the nature of the receptor sequence on axon guidance in neurons that activate the modified P2 allele. If the odorant receptor were the sole determinant of axon targeting, we would expect that the M12→P2 neurons would target to the M12 glomeruli. If the odorant receptor were to play no role in the guidance process, cells activating the modified P2 allele that encodes the M12 receptor should maintain their projections to the wild-type P2 glomeruli. An intermediate model in which the olfactory receptor is one component in a more complex guidance process predicts that M12→P2 neurons will project to glomeruli distinct from either the wild-type P2 or M12 glomeruli. We observe that substitution of P2 coding sequences by M12 DNA results in the convergence of axons to topographically fixed glomeruli distant from the wild-type M12 glomeruli, but quite close to the wild-type P2 glomeruli. Since the M12→P2 neurons are likely to differ from P2 expressing cells only in the nature of the sequences at the P2 receptor locus, our data suggest that the olfactory receptor may be one determinant in the guidance process. However, the olfactory receptor cannot be the sole determinant governing the formation of a precise topographic map.

What is the role of the odorant receptor in the guidance process? The odorant receptor may influence the sites of axonal convergence by one of two mechanisms. The odorant receptor may be expressed in both dendrites and axons and may recognize guidance cues elaborated by cells of the bulb independent of receptor activation in the dendrites. Alternatively, in an activity-dependent mechanism, the synchronous firing of subsets of olfactory neurons expressing a given receptor could result in the segregation of M12→P2 neurons at sites close to, but distinct from P2 expressing neurons. We observe that the M12→P2 glomeruli are precisely positioned relative to the P2 glomeruli in all animals examined. Although coordinated activity of sensory neurons can result in the segregation of the M12→P2 axons at a glomerulus distinct from that of the P2 axons, it is difficult to invoke activity-dependent processes to precisely position these glomeruli with respect to one another. Thus, our data suggest that the odorant receptors may play an instructive role in the guidance process as one of a complement of guidance receptors involved in the generation of a precise topographic map.

These results suggest that a combination of guidance receptors elaborated on axon termini may recognize distinct sets of guidance cues expressed by the olfactory bulb. These guidance receptors may act either together or sequentially to generate a precise olfactory sensory map. The observation that neurons expressing a given olfactory receptor project to topographically fixed loci in all animals suggest that there must be a tight linkage between the choice of an odorant receptor and the expression of specific guidance receptors. Mechanisms by which neurons express only one of a thousand olfactory receptor genes are likely to involve a hierarchy of controls that may coordinately regulate the expression of odorant receptors as well as guidance receptors. For example, zonally restricted transcription factors that regulate the expression of odorant receptors may coordinately regulate the expression of a distinct set of guidance receptors. An additional level of control may be provided by the clustering of receptor genes in linked arrays at multiple chromosomal loci (Ben-Arie et al., 1994; Sullivan et al., 1996). Activation of a specific array may be associated with the coordinate expression of specific guidance receptors. In support of this suggestion, we observe that the M12→P2 glomeruli are extremely close to the wild-type P2 glomeruli. This observation suggests the possibility that transcriptional control of P2 expression may be coordinated with the choice of a combination of guidance receptors that drive axons to the vicinity of the P2 glomeruli independent of the nature of the olfactory receptor sequences at the P2 locus. Once axons have arrived within this local domain, they might then employ the odorant receptors as guidance receptors to find the appropriate target. Thus, axons from neurons expressing the P2 receptor would converge at one glomerular location, whereas axons from cells expressing the M12 receptor from the M12→P2 allele (although not normally present in this local domain) would converge on a different, spatially fixed glomerulus. In this manner, the odorant receptor itself may be an instructive determinant in the guidance process.

Experimental Procedures

Construction of tau-lacZ Plasmids

LTNL

pgk-neo (Adra et al., 1987) in pGEM7 was cut at the 3′ end with HindIII and SacI and the following oligonucleotide, as well as the complementary oligonucleotide, was inserted to generate plasmid neo-3′loxP: 5′AGCTTATAACTTCGTATAATGTATGCTATACGAAGT TATTTAATTAATCTAGAGAGCT3′. This sequence contains, respectively, a HindIII site, a 34 nt *loxP* site (Hoess et al., 1982), a PacI site, an XbaI site, and a SacI site. Plasmid pIC19R (Mansour et al., 1988) containing HSV-*tk* (McKnight, 1980) was cut at the 5′ end with XhoI and the following oligonucleotide, as well as the complementary oligonucleotide, was inserted to generate plasmid 5′loxP-tk: 5′TCGAGTCTAGAATAACTTCGTATAATGTATGCTATACGAAGT TATG3′. This oligonucleotide contains, respectively, a XhoI site, an XbaI site, a 34 nt *loxP* site, and a SalI site (the latter site is compatible with an XhoI site, but ligation destroys both sites). The 5′loxP-tk insert was released by XhoI and SalI as a 2.0 kb fragment and ligated into the XhoI site at the 5′ end of neo-3′loxP, generating plasmid LTNL. The 3.9 kb insert of LTNL, containing a PacI site at the 3′ end, can be released from pGEM7 as an XbaI fragment.

ETLpA-/LTNL

The IRES from the encephalomyocarditis virus was subcloned into pBluescript as a 0.6 kb EcoRI–BamHI fragment, derived from plasmid pWH10 (Kim et al., 1992). The GG nucleotides 5′ of the ATG start codon of the bovine tau coding sequence (Butner and Kirschner, 1991) were converted to CC by PCR to generate an NcoI site, using τ-*lacZ* in KS$^+$ (Callahan and Thomas, 1994). The 235 nt NcoI–NotI 5′ fragment of tau was inserted into the subcloned IRES. A PacI site was inserted at the 5′ end of the IRES-5′ tau plasmid via ligation of an XhoI–PacI–EcoRI oligonucleotide linker. The 5.25 kb NotI fragment of τ-*lacZ* in KS$^+$ was subsequently inserted into this plasmid, generating plasmid ETL. The lacZ sequences followed by the SV40 polyadenylation signal were excised from ETL as a 4.25 kb BamHI fragment and replaced by the 3.0 kb BamHI fragment from plasmid pMC1871 (Pharmacia), containing the lacZ coding sequence without any polyadenylation signal, generating plasmid ETLpA-. The LTNL cassette was inserted as an XbaI fragment, generating plasmid ETLpA-/LTNL. The insert can be excised from pBluescript as an 8.8 kb PacI fragment. Another variant was constructed in which the insert can be excised with AscI.

TL/LTNL

Plasmid ETL was cut with PacI and NcoI, and the IRES sequences were replaced with a PacI–EcoRI–NcoI olignucleotide linker, generating plasmid TL. The 3.9 kb XbaI insert of LTNL was inserted to generate plasmid TL/LTNL. The insert can be excised from pBluescript as a 9.4 kb PacI fragment.

The accuracy of the sequences generated by PCR or oligonucleotide linker insertion, as well as of all junctional sequences, was confirmed by DNA sequencing. These plasmids can be obtained from P. M.

Generation of Targeted Mutations

OMP-tau-lacZ

Genomic clones containing *OMP* were isolated from a phage library derived from a 129 mouse (Stratagene). The 0.67 kb NcoI fragment comprising the sequences between the NcoI site at the start codon of the intronless *OMP* gene (0.39 kb) to the NcoI site in the 3′ nontranslated region (0.28 kb), was deleted and replaced with a PacI linker. The PacI insert of TL/LTNL was ligated to generate targeting vector OMP-KO-2, which consists of 4.5 kb of 3′ flanking sequence and 6 kb of 3′ flanking sequence. A PmeI site was inserted 3′ of the SphI site in OMP-KO-2 to linearize the plasmid. Linearized plasmid (35 μg) was used to electroporate 30 × 10^6 D3 ES cells (Doetschman et al., 1985) at 800 V and 3 μF with a Bio-Rad Gene Pulser. Cells were cultured on mitomycin C inactivated primary embryonic fibroblasts derived from *neo*-resistant transgenic mice (Gossler et al., 1986). Selection with 150 μg/ml of G418 was initiated after 24 hr, and colonies were picked after 7–8 days. Genomic DNA was cut with EcoRI and hybridized with an external 5′ OMP probe. Clone B38 was expanded and electroporated with circular pB185 (GIBCO–Life Technologies). Cells were grown and replated for six days, after which they were plated at low density and selected with 2 μM ganciclovir. Colonies were picked after 5–6 days; genomic DNA was cut with BamHI and hybridized to the 3′ OMP probe (1.32 kb NcoI–BamHI fragment). B38/CreA5 was injected into C57Bl/6 blastocysts to produce germline chimeras. Mice are in a mixed (129 × C57Bl/6) background.

P2-IRES-tau-lacZ

Genomic clones containing P2 were isolated from a phage library constructed from a Yeast Artificial Chromosome containing the P2 gene, of C57Bl/6 origin. Recombinant PCR was employed to insert the sequences encoding the human c-*myc* epitope between the second and third codon of P2 and to introduce an AscI restriction site three nucleotides 3′ of the P2 stop codon. The ETLpA-/LTNL cassette was inserted as an AscI fragment to generate plasmid P2-KO-13, which consists of 1.4 kb 5′ flanking sequence and 5.4 kb of 3′ flanking sequence. The plasmid was linearized at the 5′ XhoI site. Targeting and Cre-excision were performed as for OMP, except that E14 cells (Hooper et al., 1987) were used. Genomic DNA from P2-KO-13 transfected, E14 derived clones was cut with NcoI and hybridized with a 5′ external probe. Genomic DNA from pBS185 transfected, targeted clones was cut with HindIII and hybridized with the 3′ P2 probe (0.6 kb Xba–BamHI fragment). The *myc* epitope sequence was not present in either of the four targeted ES clones, suggesting that the 5′ crossing over event occurred within the 1 kb P2 coding sequence. Mice are in a mixed (129 × C57Bl/6) background.

M12→P2-IRES-tau-lacZ

The M12 coding sequence was modified by recombinant PCR to introduce 27 nucleotides encoding the hemagglutinin epitope tag, between the second and third codon. Via recombinant PCR and oligonucleotide linker insertion a PacI site was created at the 5′ end of the M12 coding sequence, and AscI and PacI restriction sites in tandem at the 3′ end. A PacI restriction site was introduced immediately 5′ of the start codon of P2, in a plasmid containing also a PacI site immediately 3′ of the stop codon; cutting with PacI and religation created a plasmid in which the P2 coding sequences are deleted neatly from start to stop codon. The M12 coding sequence was cloned in this plasmid as a PacI restriction fragment, and ET-LpA-/LTNL was subsequently ligated as an AscI restriction fragment. Gene targeting, Cre-recombination, and generation of chimeras were performed as described for P2-IRES-tau-lacZ.

X-Gal Staining

For whole mounts, tissues were fixed for 30 min on ice with 100 mM phosphate buffer (pH 7.4), 4% paraformaldehyde, 2 mM $MgSO_4$, and 5 mM EGTA; washed with buffer A (100 mM phosphate buffer [pH 7.4], 2 mM $MgCl_2$, and 5 mM EGTA), once for 5 min, and once for 30 min, at room temperature; followed by two washes of 5 min at room temperature with buffer B (100 mM phosphate buffer [pH 7.4], 2 mM $MgCl_2$, 0.01% sodium desoxycholate, and 0..02% Nonidet P40). The blue precipitate was generated by exposure in the dark at 37°C to buffer C (buffer B, with 5 mM potassium-ferricyanide, 5 mM potassium-ferrocyanide, and 1 mg/ml of X-Gal). For sections, the bulb was frozen in OCT (Miles), 10 μm sections were cut with a Hacker-Bright cryostat, stained with X-Gal, and counterstained with neutral red after dehydration.

In Situ Hybridization

In situ hybridization was carried out with either a ^{33}P- or a digoxigenin-labeled riboprobe specific for the coding region of P2 (0.7 kb long), as described previously in detail (Vassar et al., 1993, 1994).

Acknowledgments

We thank Leonardo Belluscio and Ali Hemmati-Brivanlou for advice; Jennifer Nuñez, Margarita Jovel, Jie Pan, and Guo-Fang Hu for technical assistance; Chris Callahan and John Thomas for sharing tau-lacZ prior to publication; Hee-Sup Shin for the IRES; Tom Jessell for critically reviewing the manuscript; and Phyllis Kisloff for preparing the manuscript. This work was supported by the Howard Hughes Medical Institute and by grants from the National Institutes of Health (5 PO1 CA23767 and 5 P50 MH 50733 [R. A.]). P. M. is a Searle Scholar. Address correspondence to R. A. (e-mail address: ra27@columbia.edu). Requests for the tau-lacZ plasmids should be addressed to P. M. (e-mail address: mombaer@rockvax.rockefeller.edu).

Received August 28, 1996; revised September 24, 1996.

References

Adra, C.N., Boer, P.H., and McBurney, M.W. (1987). Cloning and expression of the mouse pgk-1 gene and the nucleotide sequence of its promoter. Gene *60*, 65–74.

Ben-Arie, N., Lancet, D., Taylor, C., Khen, M., Walker, N., Ledbetter, D.H., Carrozzo, R., Patel, K., Sheer, D., Lehrach, H., and North, M.A. (1994). Olfactory receptor gene cluster on human chromosome 17: possible duplication of an ancestral receptor repertoire. Hum. Mol. Genet. *3*, 229–235.

Buck, L.B. (1996). Information coding in the vertebrate olfactory system. Annu. Rev. Neurosci. *19*, 517–544.

Buck, L., and Axel, R. (1991). A novel multigene family may encode odorant receptors: a molecular basis for odor recognition. Cell *65*, 175–187.

Buiakova, O.I., Krishna, N.S, Getchell, T.V., and Margolis, F.L. (1994). Human and rodent OMP genes: conservation of structural and regulatory motifs and cellular localization. Genomics *20*, 452–462.

Butner, K.A., and Kirschner, M.W. (1991). Tau protein binds to microtubules through a flexible array of distributed weak sites. J. Cell. Biol. *115*, 717–730.

Callahan, C.A., and Thomas, J.B. (1994). Tau-beta-galactosidase, an axon-targeted fusion protein. Proc. Natl. Acad. Sci. USA *91*, 5972–5976.

Chess, A., Simon, I., Cedar, H., and Axel, R. (1994). Allelic inactivation regulates olfactory receptor gene expression. Cell *78*, 823–834.

Constantine-Patton, M., Cline, H.T., and Debski, E. (1990). Patterned activity, synaptic convergence, and the NMDA receptor in developing visual pathways. Annu. Rev. Neurosci. *13*, 129–154.

Doetschman, T.C., Eistetter, H., Katz, M., Schmidt, W., and Kemler, R. (1985). The in vitro development of blastocyst-derived embryonic stem cell lines: formation of visceral yolk sac, blood islands and myocardium. J. Embr. Exp. Morph. *87*, 27–45.

Farbman, A.I., and Margolis, F.L. (1980). Olfactory marker protein during ontogeny: immunohistochemical localization. Dev. Biol. *74*, 205–215.

Goodman, C.S., and Shatz, C.J. (1993). Developmental mechanisms that generate precise patterns of neuronal connectivity. Cell *72*, Neuron *10* (Suppl.), 77–98.

Gossler, A., Doetschman, T., Korn, R., Serfling, E., and Kemler, R. (1986). Transgenesis by means of blastocyst-derived embryonic stem cell lines. Proc. Natl. Acad. Sci. USA *83*, 9065–9069.

Hoess, R.H., Ziese, M., and Sternberg, N. (1982). P1 site-specific recombination: nucleotide sequence of the recombining sites. Proc. Natl. Acad. Sci. USA *79*, 3398–3402.

Hooper M., Hardy, K., Handyside, A., Hunter, S., and Monk, M. (1987). HPRT-deficient (Lesch-Nyhan) mouse embryos derived from germline colonization by cultured cells. Nature *326*, 292–295.

Imamura, K., Mataga, N., and Mori, K. (1992). Coding of odor molecules by mitral/tufted cells in rabbit olfactory bulb. I. Aliphatic compounds. J. Neurophysiol. *68*, 1986–2002.

Katoh, K., Koshimoto, H., Tani, A., and Mori, K. (1993). Coding of odor molecules by mitral/tufted cells in rabbit olfactory bulb. II. Aromatic compounds. J. Neurophysiol. *70*, 2161–2175.

Kauer, J.S., Senseman, D.M., and Cohen, L.B. (1987). Odor-elicited activity monitored simultaneously from 124 regions of the salamander olfactory bulb using a voltage-sensitive dye. Brain Res. *418*, 255–261.

Kim, D.G., Kang, H.M., Jang, S.K., and Shin, H.S. (1992). Construction of a bifunctional mRNA in the mouse by using the internal ribosomal entry site of the encephalomyocarditis virus. Mol. Cell. Biol. *12*, 3636–3643.

Lancet, D., Greer, C.A., Kauer, J.S., and Shepherd, G.M. (1982). Mapping of odor-related neuronal activity in the olfactory bulb by high-resolution 2-deoxyglucose autoradiography. Proc. Natl. Acad. Sci. USA *79*, 670–674.

Levy, N.S., Bakalyar, H.A., and Reed, R.R. (1991). Signal transduction in olfactory neurons. J. Steroid. Biochem. Mol. Biol. *39*, 633–637.

Mansour, S.L., Thomas, K.R., and Capecchi, M.R. (1988). Disruption of the proto-oncogene int-2 in mouse embryo-derived stem cells: a general strategy for targeting mutations to non-selectable genes. Nature *336*, 348–352.

McKnight, S.L. (1980). The nucleotide sequence and transcript map of the herpes simplex virus thymidine kinase gene. Nucleic Acids Res. *8*, 5949–5964.

Mombaerts, P. (1996). Targeting Olfaction. Curr. Opin. Neurobiol. *6*, 481–486.

Mori, K., Mataga, N., and Imamura, K.J. (1992). Differential specificities of single mitral cells in rabbit olfactory bulb for a homologous series of fatty acid odor molecules. J. Neurophysiol. *67*, 786–789.

Mountford, P.S., and Smith, A.G. (1995). Internal ribosome entry sites and dicistronic RNAs in mammalian transgenesis. Trends Genet. *11*, 179–184.

Ngai, J., Chess, A., Dowling, M.M., Necles, N., Macagno, E.R., and

Axel, R. (1993). Coding of olfactory information: topography of odorant receptor expression in the catfish olfactory epithelium. Cell *72*, 667–680.

Parmentier, M., Libert, F., Schurmans, S., Schiffmann, S., Lefort, A., Eggerickx, D., Ledent, C., Mollereau, C., Gérard, D., Perret, J., et al. (1992). Expression of members of the putative olfactory receptor gene family in mammalian germ cells. Nature *355*, 453–455.

Ressler, K.J., Sullivan, S.L., and Buck, L.B. (1993). A zonal organization of odorant receptor gene expression in the olfactory epithelium. Cell *73*, 597–609.

Ressler, K.J., Sullivan, S.L., and Buck, L.B. (1994). Information coding in the olfactory system: evidence for a stereotyped and highly organized epitope map in the olfactory bulb. Cell *79*, 1245–1255.

Royet, J.P., Souchier, C., Jourdan, F., and Ploye, H.J. (1988). Morphometric study of the glomerular population in the mouse olfactory bulb: numerical density and size distribution along the rostrocaudal axis. J. Comp. Neurol. *270*, 559–568.

Sauer, B., and Henderson, N. (1990). Targeted insertion of exogenous DNA into the eukaryotic genome by the Cre recombinase. New Biol. *2*, 441–449.

Shepherd, G.M. (1994). Discrimination of molecular signals by the olfactory receptor neuron. Neuron *13*, 771–790.

Stewart, W.B., Kauer, J.S., and Shepherd, G.M. (1979). Functional organization of rat olfactory bulb analysed by the 2-deoxyglucose method. J. Comp. Neurol. *185*, 715–734.

Strotmann, J., Wanner, I., Krieger, J., Raming, K., and Breer, H. (1992). Expression of odorant receptors in spatially restricted subsets of chemosensory neurones. Neuroreport *3*, 1053–1056.

Strotmann, J., Wanner, I., Helfrich, T., Beck, A., and Breer, H. (1994). Rostrocaudal patterning of receptor expressing neurones in the rat nasal cavity. Cell Tissue Res. *278*, 11–20.

Strotmann, J., Wanner, I., Helfrich, T., and Breer, H. (1995). Receptor expression in olfactory neurons during rat development: in situ hybridization studies. Eur. J. Neurosci. *7*, 492–500.

Sullivan, S.L., Bohm, S., Ressler, K.J., Horowitz, L.F., and Buck L.B. (1995). Target-independent pattern specification in the olfactory epithelium. Neuron *15*, 779–789.

Sullivan, S.L., Adamson, M.C., Ressler, K.J., Kozak, C.A., and Buck. L.B. (1996). The chromosomal distribution of mouse odorant receptor genes. Proc. Natl. Acad. Sci. USA *93*, 884–888.

Vassar, R., Ngai, J., and Axel, R. (1993). Spatial segregation of odorant receptor expression in the mammalian olfactory epithelium. Cell *74*, 309–318.

Vassar, R., Chao, S.K., Sitcheran, R., Nuñez, J.M., Vosshall, L.B., and Axel. R. (1994). Topographic organization of sensory projections to the olfactory bulb. Cell *79*, 981–991.

Woolsey, T.A. (1990). Peripheral alteration and somatosensory development. In Development of Sensory Systems in Mammals, E.J. Coleman, ed. (New York: Wiley), pp. 461–516.